Molecular Biology of the Cell
Vol. 19, 3769–3781, September 2008

The SNAP-25 Linker as an Adaptation Toward Fast Exocytosis

Gábor Nagy,*†‡ Ira Milosevic,*‡§ Ralf Mohrmann,* Katrin Wiederhold,‖ Alexander M. Walter,* and Jakob B. Sørensen*

*Molecular Mechanism of Exocytosis, Max Planck Institute for Biophysical Chemistry, 37077 Göttingen, Germany; and ‖Department of Neurobiology, Max Planck Institute for Biophysical Chemistry, 37077 Göttingen, Germany

Submitted December 6, 2007; Revised May 23, 2008; Accepted June 18, 2008
Monitoring Editor: Thomas F. J. Martin

The assembly of four soluble *N*-ethylmaleimide-sensitive factor attachment protein receptor domains into a complex is essential for membrane fusion. In most cases, the four SNARE-domains are encoded by separate membrane-targeted proteins. However, in the exocytotic pathway, two SNARE-domains are present in one protein, connected by a flexible linker. The significance of this arrangement is unknown. We characterized the role of the linker in SNAP-25, a neuronal SNARE, by using overexpression techniques in synaptosomal-associated protein of 25 kDa (SNAP-25) null mouse chromaffin cells and fast electrophysiological techniques. We confirm that the palmitoylated linker-cysteines are important for membrane association. A SNAP-25 mutant without cysteines supported exocytosis, but the fusion rate was slowed down and the fusion pore duration prolonged. Using chimeric proteins between SNAP-25 and its ubiquitous homologue SNAP-23, we show that the cysteine-containing part of the linkers is interchangeable. However, a stretch of 10 hydrophobic and charged amino acids in the C-terminal half of the SNAP-25 linker is required for fast exocytosis and in its absence the calcium dependence of exocytosis is shifted toward higher concentrations. The SNAP-25 linker therefore might have evolved as an adaptation toward calcium triggering and a high rate of execution of the fusion process, those features that distinguish exocytosis from other membrane fusion pathways.

INTRODUCTION

The soluble *N*-ethylmaleimide-sensitive factor attachment protein receptors (SNAREs) are central to vesicular trafficking (Fasshauer, 2003; Jahn and Scheller, 2006; Rizo *et al*., 2006) and characterized by a stretch of 60–70 amino acids, known as the SNARE motif (Terrian and White, 1997; Weimbs *et al*., 1997). The assembly of four SNARE domains into a coiled-coil bundle is a general mechanism in fusion of intracellular membrane compartments. The bundle is held together by layers of hydrophobic interaction, with the exception of the middle layer (layer "0"), which is formed by an arginine and three glutamines (Sutton *et al*., 1998). The SNARE domains can be subdivided into four homologous groups, named after their contribution to the zero layer: R, Qa, Qb, and Qc (Fasshauer *et al*., 1998b). SNARE assembly requires the participation of one domain from each group, resulting in a certain degree of specificity (McNew *et al*., 2000; Scales *et al*., 2000a).

In most cases, the four SNARE-domains are encoded by separate membrane-targeted proteins, but the SNAREs driving the fusion of vesicles with the plasma membrane (exocytosis) are special in that three proteins provide the four domains (Weimbs *et al*., 1998; Fukuda *et al*., 2000). One of the SNAREs in this pathway, exemplified by the best-known isoform synaptosomal-associated protein of 25 kDa (SNAP-25), seems to have been created by fusion of the Qb and Qc SNAREs. This arrangement necessitates a flexible linker, which runs back along the complex from the C-terminal end of the first (Qb) SNARE-domain and connects to the N-terminal end of the second SNARE-domain (Qc). This antiparallel linker is a special feature of exocytotic SNARE complexes in eukaryotic organisms from yeast to human.

The only function so far ascribed to the linker domain is the membrane-targeting of SNAP-25 and SNAP-23 through the palmitoylation of four to five cysteine residues in the N-terminal end of the linker (Gonzalo *et al*., 1999; Loranger and Linder, 2002). However, other members of the family (SNAP-29, SNAP-46, Sec9, and SPO20) lack linker cysteines. It remains controversial whether palmitoylation is needed for the function of SNAP-25 in exocytosis, or only for membrane targeting, and it is unknown whether the linker plays any other, more active role in determining the special features that distinguish exocytosis from other membrane fusion reactions: calcium-triggering and a high rate of execution of the fusion process.

Ca^{2+}-triggered exocytosis from *Snap-25* null mouse chromaffin cells is nearly abolished, but it can be rescued by viral expression of SNAP-25 isoforms (Sorensen *et al*., 2003b).

This article was published online ahead of print in *MBC in Press* (http://www.molbiolcell.org/cgi/doi/10.1091/mbc.E07–12–1218) on June 25, 2008.

‡ These authors contributed equally to this work.

Present addresses: † National Centre for Stereotactic Radiosurgery, Royal Hallamshire Hospital, Sheffield S10 2JF, United Kingdom; § Department of Cell Biology, Yale University, School of Medicine, New Haven, 06510 CT.

Address correspondence to: Jakob B. Sørensen (jsoeren@gwdg.de).

Abbreviations used: LDCV, large dense-core vesicle; RRP, readily-releasable pool; SNAP-25, synaptosome-associated protein of 25 kDa; SNARE, soluble *N*-ethylmaleimide-sensitive factor attachment protein receptors; SRP, slowly releasable pool; WT, wild type.

Here, we used this approach and fast electrophysiological techniques to address the role of the SNAP-25 linker domain in exocytosis. By mutating linker-cysteines in SNAP-25 and substituting the SNAP-23 linker for its SNAP-25 counterpart, we verify the function of cysteines in membrane targeting, and we show that the cysteine-containing part of the SNAP-25 and SNAP-23 linker is interchangeable. However, a short 10-amino acid stretch at the C-terminal end of the SNAP-25 linker is necessary for fast calcium triggering of exocytosis. These data establish the SNAP-25 linker as an integral part of the membrane fusion machinery, and they suggest that the arrangement of the Qa and Qb motifs in one protein together with a linker is an adaptation toward fast exocytosis.

MATERIALS AND METHODS

Cell Culture and Expression Constructs

Snap-25 null animals and control littermates were obtained by crossing heterozygotes and recovered by Cesarean section at embryonic days 17–19. Primary culture of mouse chromaffin cells was prepared and cultured as described previously (Sorensen *et al*., 2003b). SNAP-25a cysteine mutants and SNAP-25a/SNAP-23 chimeras were produced by polymerase chain reaction (PCR), and all constructs were verified by DNA sequencing. Semliki Forest virus particles expressing mutant/chimera together with enhanced green fluorescent protein from a bicistronic message were generated as described (Ashery *et al*., 1999). For bacterial expression of the SNAP-25a and SNAP-23 linker domain constructs, corresponding DNAs were cloned into a pET28a vector via the NdeI/EcoRI cleavage sites.

Immunofluorescence on Plasma Membrane Sheets

Plasma membrane sheets were generated 6 h after viral infection of mouse embryonic chromaffin cells and subsequently fixed, washed, and blocked as described previously (Nagy *et al*., 2005). The membrane sheets were incubated with the primary antibodies (mouse anti-SNAP-25, dilution 1:100; rabbit anti-syntaxin 1, dilution 1:100; Synaptic Systems, Göttingen, Germany) for 3 h and subsequently with cyanine (Cy)3- and Cy5-coupled secondary antibodies for 60 min (dilutions 1:200; Jackson ImmunoResearch Laboratories, West Grove, PA). All antibodies were diluted in phosphate-buffered saline (PBS) containing 1% bovine serum albumin. 1-(4-Trimethyl-aminiumphenyl)-6-phenyl-1,3,5-hexatriene (Invitrogen, Carlsbad, CA) was used for visualizing the plasma membrane. Samples were examined with an Axiovert 100TV fluorescence microscope (Carl Zeiss, Oberkochen, Germany) with a 100 × 1.4 numerical aperture plan achromate objective by using appropriate fluorescence filters (Carl Zeiss). Images were taken with a back-illuminated frame transfer charge-coupled device camera (512 × 512-NTE Chip, 24- × 24-μm pixel size; Scientific Instruments, Monmouth Junction, NJ) with a magnifying lens (2.5× Optovar). Digital image analysis was performed using MetaMorph software (Molecular Devices, Sunnyvale, CA). To quantify fluorescence intensity, a region-of-interest was defined on the randomly selected membrane and transferred to the other channels. The fluorescence intensity was calculated by measuring the average intensity of the area and subtracting the local background. At least 10 membrane sheets from each animal were analyzed, and the mean value for each animal was used to calculate population mean and SEM (5–13 animals per condition). Correlative features of fluorescent spots were analyzed as described in Nagy *et al.* (2005).

Immunoblotting

Bovine chromaffin cell preparation was performed essentially as described previously (Nagy *et al*., 2002). The primary antibodies used were rabbit anti-SNAP-25 (1:3000; catalog no. 111 002, Synaptic Systems, Göttingen, Germany) and anti-valosin–containing protein (VCP, 1:3000; catalog no, ab11433, Abcam, Cambridge, United Kingdom), which was used as a loading control. Equal amounts of proteins were separated on a 4–20% SDS-polyacrylamide gel (Ready Gel; Bio-Rad Laboratories, Hercules, CA), and they were blotted onto nitrocellulose membranes (Amersham Hybond-ECL; GE Healthcare Bio-Sciences, Uppsala, Sweden). After incubation with secondary antibodies (goat anti-rabbit/anti-mouse horseradish peroxidase-conjugated immunoglobulin G, 1:2000; Jackson ImmunoResearch Laboratories), the membranes were washed three times and incubated in ECL Western blotting detection reagent (SuperSignal, West Pico; Pierce Chemical, Rockford, IL). Chemiluminescence was detected by a digital gel documentation system; quantification was performed by densitometry using ImageJ software (National Institutes of Health, Bethesda, Maryland). The expression level was corrected for the infection efficiency, which was estimated as the ratio of green fluorescent protein (GFP)-expressing cells to the total cell number.

Ca^{2+} Uncaging and Measurements, Electrophysiology, and Electrochemistry

Mouse chromaffin cells were infected and 5–8 h were allowed for expression of wild-type and mutant constructs in the same preparations. Whole-cell patch clamp, ratiometric intracellular calcium ($[Ca^{2+}]_i$) measurements, flash photolysis of caged Ca^{2+}, and amperometry and membrane capacitance measurements were performed as described previously (Nagy *et al*., 2002). Data were analyzed using Igor Prosoftware (Wavemetrics, Lake Oswego, OR). Pool sizes and fusion time constants were obtained by fitting a sum of exponential functions to individual capacitance traces; data are presented as mean ± SEM. The significance was tested using nonparametric Mann–Whitney test.

Protein Expression and Purification

The expression constructs for cysteine-free SNAP-25A (C84S, C85S, C90S, C92S; amino acids [aa] 1–206), for the syntaxin 1a SNARE motif (SyxH3; aa 180–262), and for synaptobrevin 2 (Syb; aa 1–96) have been described previously (Fasshauer *et al*., 1998a).

For expression of SNAP-25a linker peptide (NKLKSSDAYKKAWGNNQDGVVASQPARVVDEREQMAISGGFIRRVTNDARE) and SNAP-23 linker peptide (NRTKNFESGKNYKATWGDGGDNSPSNVVSKQPSRITNGQPQQTTGAASGGYIKRITNDARE) the fragments were introduced into the pET28a plasmid between the NheI and the EcoRI sites. Protein expression was induced in *Escherichia coli* BL21(DE3) by adding 0.8 mM isopropyl-β-D-thiogalactopyranoside to a bacterial culture grown in Luria-Bertani medium to OD_{600} ~0.8. The bacteria were pelleted and resuspended in extraction buffer (500 mM NaCl, 50 mM Tris, pH 7.4, and 8 mM imidazole). Cells were sonified in the presence of 6 M urea and subsequently incubated with nickel-nitrilotriacetic acid. After 1 h at 8°C, the Ni^{2+} beads were washed with extraction buffer, and the recombinant protein was eluted with 400 mM imidazole (plus half of the extraction buffer). The His-tag was cleaved off by thrombin during overnight dialysis in 20 mM Tris, 50 mM NaCl, and 1 mM dithiothreitol, pH 7.4. After purification by ion exchange chromatography on an Äkta system (GE Healthcare Bio-Sciences) using Mono-S column (GE Healthcare Bio-Sciences), all peptides were pure as judged by SDS- polyacrylamide gel electrophoresis (PAGE) analysis. Protein concentration was determined by absorption at 280 nm, and peptides were stored at −20°C.

SDS-PAGE was carried out as described previously (Schagger *et al*., 1988). For testing SNARE-complex assembly, equimolar amounts of the SNARE proteins were incubated for one hour at room temperature. When testing for SDS resistance, samples were solubilized in SDS sample buffer (not boiled) before analysis on a 12% polyacrylamide gel.

Circular Dichroism (CD) Spectroscopy Measurements

CD measurements were performed using a Jasco model J-720 instrument (Applied Photophysics, Leatherhead, United Kingdom) by using quartz cuvettes with 1-mm pathlength (Helma, Mülheim, Germany). All experiments were carried out in 20 mM sodium phosphate buffer, pH 7.4, in the presence of 100 mM NaCl at 25°C. Liposomes (65% brain phosphatidylcholine, 30% brain phosphatidylserine, 5% phosphatidylinositol-4,5-bisphosphate were mixed in chloroform and dried; Avanti Polar Lipids, Alabaster, AL) were prepared in 20 mM Tris buffer with 100 mM NaCl, pH 7.4, by the SMART system (GE Healthcare Bio-Sciences).

RESULTS

Palmitoylation of the SNAP-25 Linker

We asked whether the palmitoylation of linker cysteines in SNAP-25 is necessary for exocytosis triggering per se, or merely plays a role for membrane targeting. To that end, we expressed SNAP-25a mutants, where one or all four linker cysteines were replaced by serines (denoted C/S mutants) using the Semliki Forest Virus expression system in chromaffin cells isolated from *Snap-25* null mice. We first investigated the targeting of SNAP-25a C/S mutants to the plasma membrane by generating plasma membrane sheets from expressing chromaffin cells. Punctate SNAP-25 immunostaining of all C/S mutants was found (Figure 1A). However, quantitatively all C/S mutants showed significant reductions in the staining compared with overexpressed WT SNAP-25a (Figure 1B). For quantification of the overall expression level we used Western blotting of bovine chromaffin cells, because cultures from a single mouse embryo do not yield sufficient protein level for quantification. It showed that all single cysteine mutants were expressed at similar level as wild-type (WT) SNAP-25a (Figure 1C; WT SNAP-

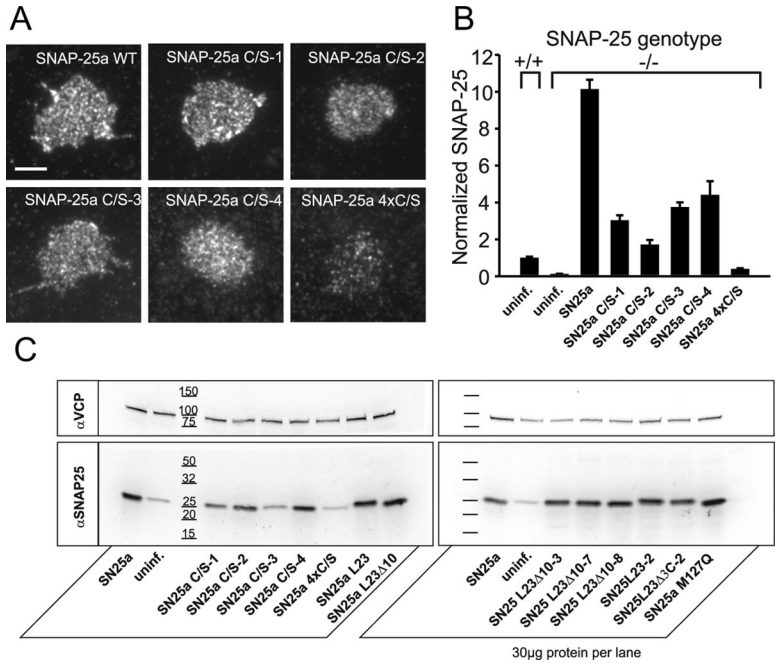

Figure 1. The linker cysteines function in membrane targeting of SNAP-25. (A) Plasma membrane sheets were generated from *Snap25* null chromaffin cells expressing SNAP-25a cysteine mutants (serine substitutions) and immunostained for SNAP-25. The SNAP-25 staining was punctate for all single cysteine mutants and WT SNAP-25a. The quadruple SNAP-25a 4xC/S mutant was present in only a few puncta on the plasma membrane sheets, indicating defective expression and/or targeting. Bar, 4 μm. (B) The staining intensities of membrane sheets were quantified. All single cysteine mutants showed significant reductions when compared with overexpressed WT SNAP-25a. SNAP-25a 4×C/S only reached 4% of the level measured after overexpression of WT SNAP-25a, indicating a severe defect in membrane targeting. Note, however, that this mutant was still present at 40% the endogenous level in nontransfected WT (+/+) cells. (C) Western blot analysis performed in bovine chromaffin cells. The overexpression level of WT SNAP-25 was around sevenfold, when correcting for infection efficiency (24–84% cells expressing), and it was significantly reduced in the SNAP-25a 4×C/S mutant (0.6- to 1-fold). Replacing the SNAP-25 linker with parts of the SNAP-23 linker, did not change the overexpression level (5.6- to 11.6-fold for different constructs, n = 3 experiments). Blotting against VCP was used as a loading control.

25a was overexpressed sevenfold, and the single cysteine mutants 4.7- to 6.9-fold, 3 experiments). The elimination of a single cysteine therefore sufficed to reduce membrane targeting to <50%, as reported previously (Washbourne *et al*., 2001). In the quadruple C/S mutation, both the overall expression level was reduced (Figure 1C; 0.6- to 1-fold expression, 3 experiments) and the amount of mutated protein on the plasma membrane, which reached only 4% of the level measured after WT overexpression (Figure 1B). Costaining of membrane sheets against syntaxin-1 showed that the level of syntaxin-1 staining was unchanged between sheets overexpressing WT SNAP-25a (308 ± 18 arbitrary units [a.u.], 4 experiments with 31–58 sheets each) and sheets overexpressing the quadrupel C/S mutant (303 ± 20 a.u., 4 experiments with 43–52 sheets each).

In addition to their function in membrane association, the palmitoylated cysteines might directly participate in exocytosis, either by assuring a tight membrane association of the Q-SNARE dimer or by positioning palmitate within the inner membrane leaflet. We therefore investigated whether ablation of single cysteines impairs the ability of SNAP-25a to mediate fast Ca^{2+}-triggered exocytosis. Secretion from mouse chromaffin cells was stimulated by flash photorelease of Ca^{2+} and monitored by simultaneous measurement of the membrane capacitance increase and amperometry to detect liberated catecholamines. All measured parameters indicated that overexpression of SNAP-25a C/S-1 and C/S-4 mutants in *Snap-25* null chromaffin cells did not impair exocytosis (Figure 2, A and B). The fast capacitance increase after flash photorelease is due to the fusion of a readily releasable pool (RRP) and a slowly releasable pool (SRP) of large dense-core vesicles (LDCVs). This is followed by a much slower, almost linear, increase as new vesicles become release-ready and fuse. During this time, the $[Ca^{2+}]_i$ is maintained at a high level by ongoing photorelease, such that the priming rate limits secretion. Through the kinetic analysis of the capacitance increase, it is possible to distinguish between vesicle pool sizes, fusion rates and sustained secretion rate (Sorensen, 2004). This analysis showed that the fast secretory burst (representing the fusion of the RRP) and the slow burst (representing the SRP) as well as the time constants of fusion from the two pools were similar to the WT situation (Figure 2, A and B). The observed increase in RRP size in the presence of C/S-1 or C/S-4 was not statistically significant. Also the sustained rate of release was unperturbed. Therefore, the ablation of single cysteines in the SNAP-25a linker region does not impair the ability of SNAP-25a to mediate fast Ca^{2+}-triggered exocytosis.

We further tested the effect of the SNAP-25a 4xC/S mutant on exocytosis. Even though the amount of this mutant on the plasma membrane was strongly impaired, the mutant still reached a plasma membrane level of 40% of endogenous expression levels, comparable with the level in SNAP-25 heterozygotes (~50%), in which no secretory defect was identified (Sorensen *et al*., 2003b) (Supplemental Figure 1). This presented an opportunity for testing whether the palmitoylation plays a role for exocytosis per se, in addition to membrane targeting. Even this mutant resulted in significant rescue of exocytosis (Figure 2, C and D). However, compared with WT protein the overall level of exocytosis was somewhat reduced, due to a reduced size of both releasable pools. In addition, the RRP fusion time constant and the time delay between the UV-flash and the start of the capacitance increase were both significantly increased, indicating that fusion triggering was negatively affected.

We next infused expressing chromaffin cells with a solution containing ~13.5 μM calcium and recorded single resolved amperometric spikes (Table 1). Because each vesicle fusion event gives rise to one amperometric spike, it is possible to estimate parameters of individual fusion events. Especially, it is possible to distinguish between the formation of a narrow fusion pore, which gives rise to a prespike "foot signal" in the amperometric recording, and the full fusion event, which results in the amperometric spike (Jackson and Chapman, 2006). Interestingly, in 4xC/S-expressing chromaffin cells the duration of the pre-spike foot signal was prolonged (Table 1). Notably, spikes in the *Snap-25* knockout cells were found to have on average shorter prespike feet (Sorensen *et al*., 2003b). This finding demonstrates that the presence of the 4xC/S mutation does not result in an inter-

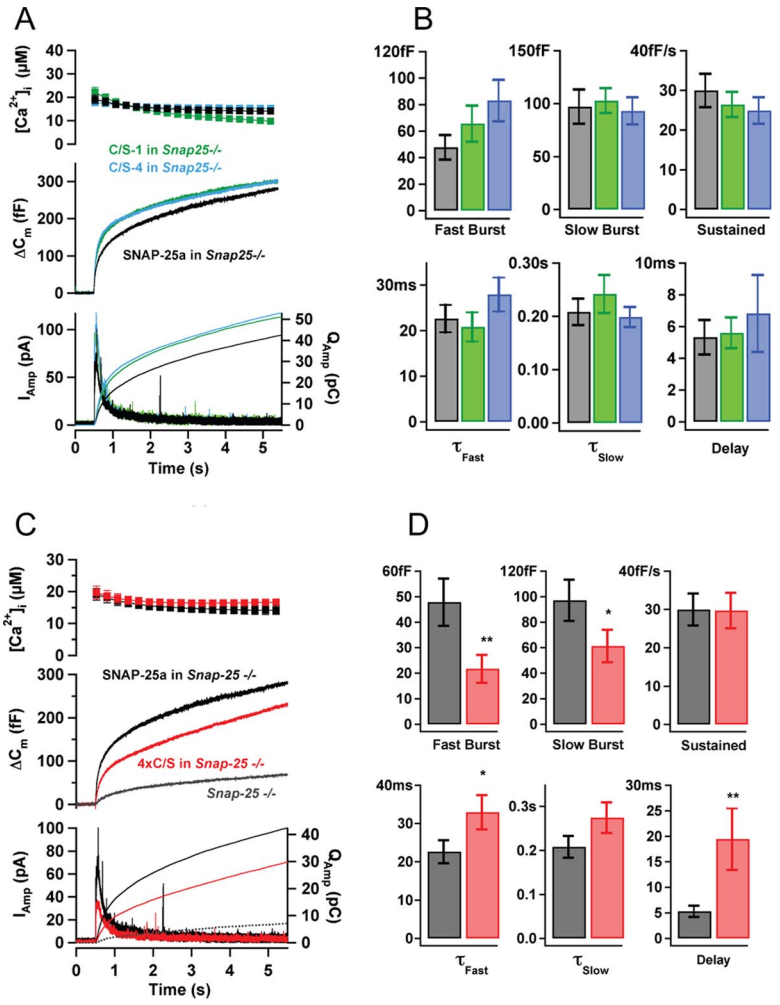

Figure 2. Function of the linker cysteines in exocytosis triggering. (A) The ablation of the first or the fourth cysteine in SNAP-25a linker does not impair the ability of SNAP-25a to mediate fast Ca^{2+}-triggered secretion. Secretion was stimulated by flash photolysis of caged Ca^{2+} (flash at arrow, $[Ca^{2+}]_i$ after the flash are shown in the top panel) and monitored by capacitance measurements (middle) and amperometry (bottom). The amperometric measurements are shown as currents (thick traces with transient increase after the flash scaled to the left ordinate axis), and the time integrals (thin monotonously increasing traces scaled to the right ordinate axis). Overexpression of SNAP-25a C/S-1 (green trace is mean of N = 38 cells) and SNAP-25a C/S-4 (blue trace is mean of n = 43 cells) mutants in *Snap-25* null chromaffin cells did not inhibit secretion as measured by both membrane capacitance and amperometry (black trace is mean of n = 41 cells expressing SNAP-25a). (B) The amplitudes (mean ± SEM) of the fast and slow burst as well as the time constants of fast and slow fusion were not significantly changed upon mutation of single cysteines. (C) Ablation of all four cysteines in the SNAP-25a linker mildly reduced the level of exocytosis (red traces, n = 47 cells expressing SNAP-25a 4xC/S; black traces, n = 41 control cells; gray traces show secretion from the *Snap-25* −/− for comparison). (D) The amplitudes (mean ± SEM) of the fast and slow burst were significantly decreased and the fast fusion time constant was significantly increased in cells overexpressing SNAP-25a 4xC/S. In addition, the secretory delay (time between photorelease of Ca^{2+} and start of capacitance increase) was significantly increased. *p < 0.05 and **p < 0.01 (Mann–Whitney test).

mediate phenotype between the *Snap-25* knockout and the wild-type situation caused by the lower expression level, but that the 4xC/S mutant causes slower secretion even on the level of individual fusion events. In addition, the 4xC/S mutation resulted in a mild and less significant increase in the charge of each spike, i.e., the quantal size.

Overall, our data show that the association of the SNARE complex with the plasma membrane through SNAP-25 palmitoylation is important for optimizing the speed of exocytosis triggering and the duration of the fusion pore.

The SNAP-25 Linker Domain Speeds Up Exocytosis Triggering

We reported previously that the expression of the ubiquitous isoform SNAP-23 in *Snap-25* null chromaffin cells supports some rescue of calcium-dependent exocytosis, but without a burst component (Sorensen *et al.*, 2003b). Here, we first repeated this experiment with similar results, and then applied stronger stimulation into the >100 μM range to investigate whether exocytosis in the presence of SNAP-23 might be shifted to higher $[Ca^{2+}]_i$ and therefore have gone undetected in previous studies. The high-Ca^{2+} stimulation elicited much larger capacitance increases that were not correlated with an amperometric signal (Supplemental Figure 2, A and B). This observation has been attributed to the SNARE-independent fusion of a population of vesicles not containing catecholamines at $[Ca^{2+}]$ >100 μM (Xu *et al.*, 1998). Therefore, only the amperometric measurements were used for assaying catecholamine release under these

Table 1. Single fusion event characteristics as measured by amperometry

	No. of cells	No. of spikes	Amplitude (pA)	$Q^{1/3}$ $(pC)^{1/3}$	Half width (ms)	Rise time (ms)	Foot duration (ms)
SNAP-25a in −/−	15	569	21.7 ± 1.7	0.53 ± 0.01	4.4 ± 0.6	0.63 ± 0.08	2.4 ± 0.4
4xC/S in −/−	13	562	27.8 ± 2.8	0.58 ± 0.02*	4.6 ± 1.0	0.73 ± 0.15	4.2 ± 0.8*
SN25L23 in −/−	9	561	21.6 ± 1.7	0.57 ± 0.02	4.6 ± 0.7	0.57 ± 0.04	2.4 ± 0.8

The table gives mean ± SEM of the cell median for each parameter. The foot duration of the quadrupel cysteine mutation was significantly longer (p = 0.017) and the charge of the spike slightly larger (p = 0.040) than in cells rescued with wild-type SNAP-25a.

* p < 0.05 (Mann–Whitney test comparing to SNAP-25a rescue).

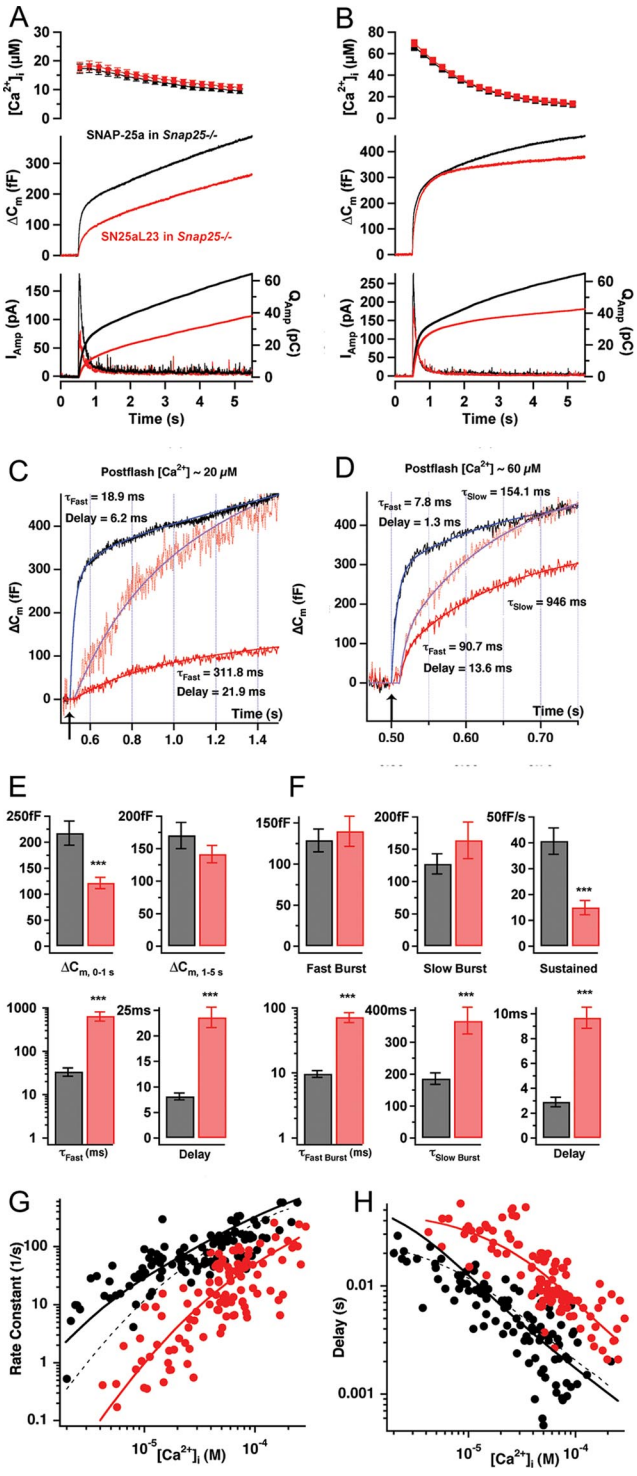

Figure 3. Overexpression of a chimeric protein (SN25aL23), where the SNAP-25 SNARE domains were fused to the SNAP-23 linker in *Snap-25* null chromaffin cells slow down exocytosis. (A) Exocytosis was stimulated and measured as described in the legend to Figure 2. The SN25aL23 chimera resulted in less exocytosis during the first 0.5 s after flash stimulation to 15–20 μM Ca^{2+}, as measured by both membrane capacitance increase and amperometry (SN25aL23, red trace is mean of 34 cells; SNAP-25a, black trace is mean of 35 cells). (B) Exocytosis within the first 0.5-s after the flash was largely rescued when stimulating to higher Ca^{2+} concentrations (60–80 μM), whereas sustained secretion was now impaired (SN25aL23, n = 26 cells; SNAP-25a, n = 26 cells). (C) Example traces from two cells stimulated to ~20 μM $[Ca^{2+}]_i$. Black trace, a *Snap-25* null cell rescued by SNAP-25a WT expression and displaying large secretion (compare with A); and red trace, example of rescue with SN25L23. Shown are also the kinetic fits to the traces (blue and red smooth lines) and the fitted kinetic parameters. For comparison under conditions of similar amplitudes, the SN25L23 trace is also shown scaled to WT amplitude at 1 s after the flash (red dotted trace). (D) Example traces from two cells stimulated to ~60 μM $[Ca^{2+}]_i$. Note expanded time scale. Color-coding as in C. The SN25L23 cell displays an exocytotic burst that could be fitted with a sum of two exponentials, with time constants 90.7 and 946 ms, respectively. The SNAP-25a WT-expressing cell features much faster secretion. (E) Kinetic analysis of responses following flash photolysis to $[Ca^{2+}]_i$ <35 μM. Because of the slowdown of exocytosis, a distinction between the fast and slow burst could not be made in the chimera. The time constant and delay were analyzed for the fastest exponential resolvable and showed massive slowdown (bottom). Red, SN25aL23 chimera; and black, WT SNAP-25a. (F) Analysis of responses to $[Ca^{2+}]_i$ >35 μM revealed that at higher $[Ca^{2+}]_i$, the fast and slow burst were recognizable in the SN25aL23 chimera at their usual amplitudes. The time constants of fusion for the fast and slow burst and the delays were all slowed down. (G) The fastest resolvable rate constant (= $1/\tau$) is plotted as a function of postflash $[Ca^{2+}]_i$. With higher $[Ca^{2+}]_i$ the rate increases (Voets, 2000). In the chimera (red symbols) the relationship is displaced to higher $[Ca^{2+}]_i$ compared with the WT (black symbols), indicating a shifted Ca^{2+} dependence of exocytosis. (H) The secretory delay (delay between flash photolysis and start of capacitance increase) as a function of postflash $[Ca^{2+}]_i$. With higher $[Ca^{2+}]_i$ the delay is shortened. In the chimera (red symbols), the relationship is shifted to higher $[Ca^{2+}]_i$. *p < 0.05, **p < 0.01, and ***p < 0.001 (Mann–Whitney test).

conditions. The high-calcium stimulations only elicited slightly more release of catecholamines than stimulation to 20–30 μM, and the secretion followed a similar time course as during flashes to 20–30 μM calcium (Supplemental Figure 2, A and B). Thus, *Snap-25* null cells do not support fast LDCV release even when expressing SNAP-23 and stimulated to $[Ca^{2+}]_i > 100$ μM.

Next, we asked whether there are any functional differences between the SNAP-23 and SNAP-25 linkers, which both act to anchor the protein in the plasma membrane. We therefore constructed chimeric proteins where the two SNARE domains from SNAP-25 were joined by the SNAP-23 linker. The crossover points of the chimera were the lysine-83(SNAP-25)/lysine-78(SNAP-23), and the glutamate-148(SNAP-25)/glutamate-153(SNAP-23) (also see Figures 4 and 5). The chimera (denoted SN25aL23) was overexpressed at similar levels as SNAP-25 WT protein (Figure 1C). When overexpressed in *Snap-25* null chromaffin cells, SN25aL23 did not fully restore secretion (Figure 3), but it led to a slowdown and a reduction in exocytosis within the first second of stimulation (Figure 3A). This partial rescue already indicates that the linker plays another role than just membrane targeting (see also below). We investigated whether stronger stimulation might recover exocytosis driven by the chimera. We increased $[Ca^{2+}]_i$ to 60–80 μM to speed up exocytosis without eliciting capacitance increases uncorrelated to amperometric charge, which typically happens at >100 μM in an all-or-none manner (Xu *et al.*, 1998). Indeed, we found that at 60–80 μM calcium, the burst of secretion within the first 0.5 s was largely restored, whether evaluated by capacitance, or by amperometric measurements (Figure 3B). The agreement between the two types of measurements shows that these recordings were not severely contaminated with fusing vesicles not containing catecholamines.

To understand the consequences for exocytosis of replacing the SNAP-25 linker with its SNAP-23 counterpart, we

performed a detailed kinetic analysis of the capacitance traces. This was done by fitting a sum of exponential functions to individual capacitance traces to identify the size of the releasable vesicle pools, RRP and SRP, together with their fusion kinetics (Figure 3, C and D). It was immediately clear that in SN25aL23-expressing cells the fusion kinetics was dramatically slowed down. At $[Ca^{2+}]_i$ <35 μM (Figure 3, A, C, and E), only a single, slow phase of exocytosis was discernible. In addition, the delay between the $[Ca^{2+}]_i$ increase and the start of the capacitance trace was much longer than in cells expressing SNAP-25 WT (Figure 3C). The fastest resolvable time constant of release was increased by a factor ~20 (Figure 3E, bottom left), whereas the secretory delay was threefold longer in the SN25aL23-expressing cells (Figure 3E, bottom right). At higher postflash $[Ca^{2+}]_i$ (Figure 3, B, D, and F), both WT and mutant cells displayed faster kinetics, as indicated by faster time constants and shorter secretory delays (Figure 3, D and F). In SN25aL23-expressing cells, two exocytotic phases were now distinguishable (Figure 3D). Strikingly, when considering cells with a calcium-increase to between 35 and 100 μM, the amplitudes of the two burst components were normal (Figure 3F, top left and middle), indicating that the releasable vesicle pool sizes were unaffected by the SNAP-23 linker. However, both the fast and slow time constant of release and the secretory delay were longer in the chimera, indicating slower exocytosis triggering with the SNAP-23 linker (Figure 3, D and F). To investigate the calcium-dependence of release, we plotted the rate constant of fast release ($= 1/\tau$) against the postflash $[Ca^{2+}]_i$ (Figure 3G). Likewise, we plotted the secretory delay against post-flash $[Ca^{2+}]_i$ (Figure 3H). In Figure 3, G and H, we included data up to 250 μM calcium, even though at >100 μM the population of noncatecholamine containing vesicles referred to earlier became dominating. However, because these vesicles fuse with a slow time constant of ~500 ms (refer to Supplemental Figure 2), it was still possible to identify the kinetics of fast burst release from these measurements, even though properties of the slow burst could not be identified. The graphical representation in Figure 3, G and H, shows that with increasing $[Ca^{2+}]_i$ the rate constant of fast release was speeded up, whereas the delays became shorter, as described previously (Voets, 2000). This calcium-dependence of secretion was shifted toward much higher concentrations in the chimeric construct containing the SNAP-23 linker. In addition to the effect on exocytosis triggering, at high $[Ca^{2+}]_i$ it became clear that the sustained rate of secretion was reduced in the chimeric construct (Figure 3, B and F, top right). This parameter has often been associated with the rate of refilling the releasable vesicle pools.

Recording of single resolved amperometric spikes did not reveal significant differences between SNAP-25a and SNAP25aL23 (Table 1), in line with the lack of significant differences following SNAP-25a and SNAP-23 overexpression (Sorensen *et al*., 2003b). This shows that a slow-down of exocytosis triggering (found both in 4xC/S mutant and in the SNAP25aL23 chimera) in some cases might correlate with a change in fusion pore duration; in other cases not. Thus, exocytosis triggering and fusion pore expansion is driven by partly different—but probably overlapping—processes.

Overall, the replacement of the SNAP-23 for the SNAP-25 linker causes a displacement of the calcium dependence of exocytosis toward much higher concentrations without changing the releasable vesicle pool sizes, and it also seems to affect slower phases of exocytosis that assay vesicle priming (see *Discussion*).

The Membrane-anchoring Parts of SNAP-25 and SNAP-23 Are Interchangeable

Even though the role of both the SNAP-25 and the SNAP-23 linker in anchoring the protein to the plasma membrane is well-established, it could not be ruled out that the chimeric SN25aL23 protein might somehow be defective in membrane-anchoring due to a mismatch between the linker and other parts of the protein. We therefore again compared the membrane anchoring, by using an antibody recognizing both SNAP-25 WT and SN25aL23. Both proteins were found in the plasma membrane after overexpression in mouse cells at 12- to 13-fold the endogeneous concentration (Figure 4, A and B). Costaining of membrane sheets against syntaxin-1 showed that the level of syntaxin-1 staining was unchanged between sheets overexpressing WT SNAP-25a (938 ± 13 a.u., 3 experiments with 34–44 sheets each) and sheets overexpressing the SN25aL23 (941 ± 20 a.u., 3 experiments with 34–48 sheets each).

Because it has been reported that SNAP-25 and SNAP-23 display different affinities for lipid rafts in PC12 cells due to a difference in the cysteine-rich linker domain (Salaun *et al*., 2005b), we also investigated the colocalization between our chimeric construct and syntaxin by using double labeling and cross-correlation analysis (Nagy *et al*., 2005). This analysis showed no major difference in the correlation coefficient, with syntaxin between SNAP-25a and SN25aL23 (the point at 0 radial distance in Figure 4C). The r decays to zero when one of the two pictures are displaced with respect to the other (radial distance >0), indicating the finite dimension of correlating domains. This analysis shows that the punctate staining pattern for syntaxin-1 and SNAP-25a overlap to the same degree as syntaxin-1 and SN25aL23.

Next, we investigated whether the SN25aL23 chimera can form SNARE-complexes, by mixing equimolar amounts of bacterially expressed and purified SNARE-proteins for 1 h at room temperature, following by SDS-PAGE (Figure 4D). Both full-length SNAP-25a, and the SN25aL23 and SN25aL23Δ3C-2 chimeras (see below), were able to form ternary SNARE-complexes with syntaxin-1 and synaptobrevin-2 (bands at arrow ~50 kDa in lanes 6–8, Figure 4D).

To identify the part of the linker responsible for the difference in exocytosis triggering, we constructed a number of chimeras (Figure 5) and tested them after overexpression in *Snap-25* null cells. The expression level of these chimeras was unchanged as compared with SNAP-25 WT protein (Figure 1C). We first investigated whether the fact that the SNAP-23 linker is 10 amino acid residues longer than the SNAP-25 linker is functionally relevant. However, a SNAP-25aL23 chimera with the extra 10 amino acids deleted (SN25AL23Δ10) still displayed what we will refer to as the "linker phenotype," i.e., incomplete rescue and a lower rate of exocytosis triggering at intermediate $[Ca^{2+}]_i$, which was overcome at higher concentrations. This is shown in Figure 6A, where we flashed to normal $[Ca^{2+}]_i$ (~20 μM, light blue traces) and very high $[Ca^{2+}]_i$ (150–200 μM, blue traces). The capacitance trace at very high $[Ca^{2+}]_i$ is contaminated by the population of noncatecholamine containing vesicles. Even though this procedure therefore does not allow detailed analysis like in Figure 3, the amperometric measurements performed in parallel (Figure 6A, bottom traces) clearly show rescue of catecholamine release at high $[Ca^{2+}]_i$, and therefore allows the fast distinction between the normal and the linker phenotype. Next, we constructed two chimeras where either the N- or the C-terminal half of the linker was from SNAP-25 (Figure 5). The former, SN25aL23Δ10-1, where the domain containing the linker cysteines was from

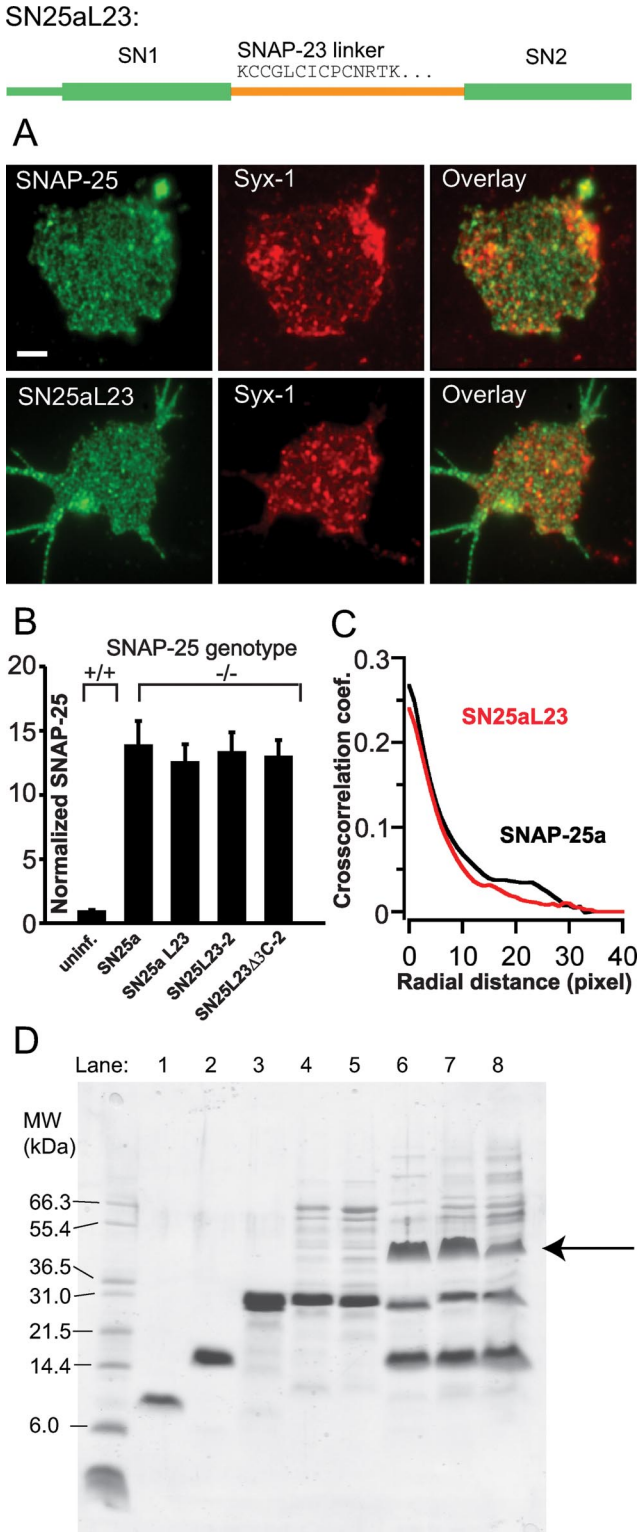

Figure 4. Normal plasma membrane targeting and in vitro SNARE-complex formation of SN25aL23 chimeras. (A) Plasma membrane sheets of *Snap-25* null chromaffin cells expressing SNAP-25a WT (top three panels) or SN25aL23 (bottom three panels) and stained against SNAP-25 and syntaxin-1 (Syx-1). Bar, 3 μm. (B) Quantification of immunostaining of isolated membrane sheets stained with a SNAP-25 antibody, which also recognizes the chimeras. The amount of SN25aL23 and some other chimeric constructs (refer to Figure 5) in the plasma membrane after overexpression is unchanged compared with SNAP-25a. (C) The cross-correlation between the SN25aL23 chimera and immunostaining for syntaxin-1 is unchanged. The abscissa gives the radial displacement of one picture with respect to the other. At displacement 0, the value is equal to the r. As the displacement gets larger, the r decays to zero, indicating the finite size of correlating domains. (D) Formation of SNARE-complexes by chimeric SNAP-25 proteins. SDS-PAGE gel (12%) of bacterially purified proteins. Lane 1, Syntaxin 1 (syx) H3 domain (aa 180–262); lane 2, synaptobrevin (syb) full-length protein (aa 1–96); lane 3, SNAP-25a 4xC/S mutant (aa 1–206); lane 4, SN25aL23 chimera (aa 1–206); lane 5, SN25aL23Δ3C-2 chimera (aa 1–206); lane 6, equimolar mixture of syx H3 + syb + SNAP25a 4xC/S mutant after incubation for 1 h, band at ~50 kDa is the ternary SNARE complex (arrow); lane 7, equimolar mixture of syx H3 + syb + SN25aL23, SNARE complex indicated (arrow); and lane 8, equimolar mixture of syx H3 + syb + SN25aL23Δ3C-2 chimera, SNARE complex at arrow.

SNAP-25, nevertheless displayed the linker phenotype (Supplemental Figure 3). Conversely, the chimera where the N-terminal part—and therefore the linker cysteines—was from SNAP-23, but the rest of the linker from SNAP-25 (SN23aL23Δ10-2) exhibited full rescue and fast secretion indistinguishable from SNAP-25a (Figure 6B).

Overall, these data show that the membrane-anchoring part of the linker containing the palmitoylated cysteines is interchangeable between SNAP-25 and SNAP-23 without implications for expression level, membrane targeting or in vitro SNARE complex formation, whereas the C-terminal part of linker surprisingly is necessary for fast exocytosis triggering.

A Short Amino Acid Stretch in the C-Terminal Half of the SNAP-25 Linker Speeds Up Exocytosis

To further narrow down the decisive part of the linker, we continued testing the chimeras displayed in Figure 5. In brief, we found that all mutants depicted in red displayed the linker phenotype, i.e., secretion like SN25aL23, whereas mutants in green had a SNAP-25a–like secretory phenotype and mutants in blue showed an intermediate phenotype. The minimum region that gave an unperturbed SNAP-25-like phenotype was a 10-amino acid stretch encompassing the positions 120–129 in SNAP-25. Chimeras including this stretch were expressed and targeted to the membrane at wild-type levels (Figures 1C and 4B) and restored secretion to normal amplitude and kinetics (Figure 7 and Supplemental Figure 4A), regardless of whether the construct included the extra seven amino acids present in SNAP-23 N-terminal of this domain. However, a chimera containing the extra three amino acids (GAA) present in SNAP-23 immediately C-terminal of the 10-amino acid stretch from SNAP-25 displayed an intermediate phenotype (Supplemental Figure 4B), showing that the domain needs to be fused directly to the remaining part of the linker, which is largely conserved between SNAP-25 and SNAP-23.

Intermediate Phenotypes Identify the Critical Properties of the SNAP-25 Linker

The critical stretch in the SNAP-25 linker consists of the amino acid sequence (in single-letter code) VVDEREQMAI, which does not to our knowledge correspond to any known consensus sequences for protein–protein interaction domains. The domain starts with two and ends with three hydrophobic amino acids, which are separated by three charged and one hydrophilic residue. In the next set of experiments, we tried to determine which properties of this domain are required for fast triggering.

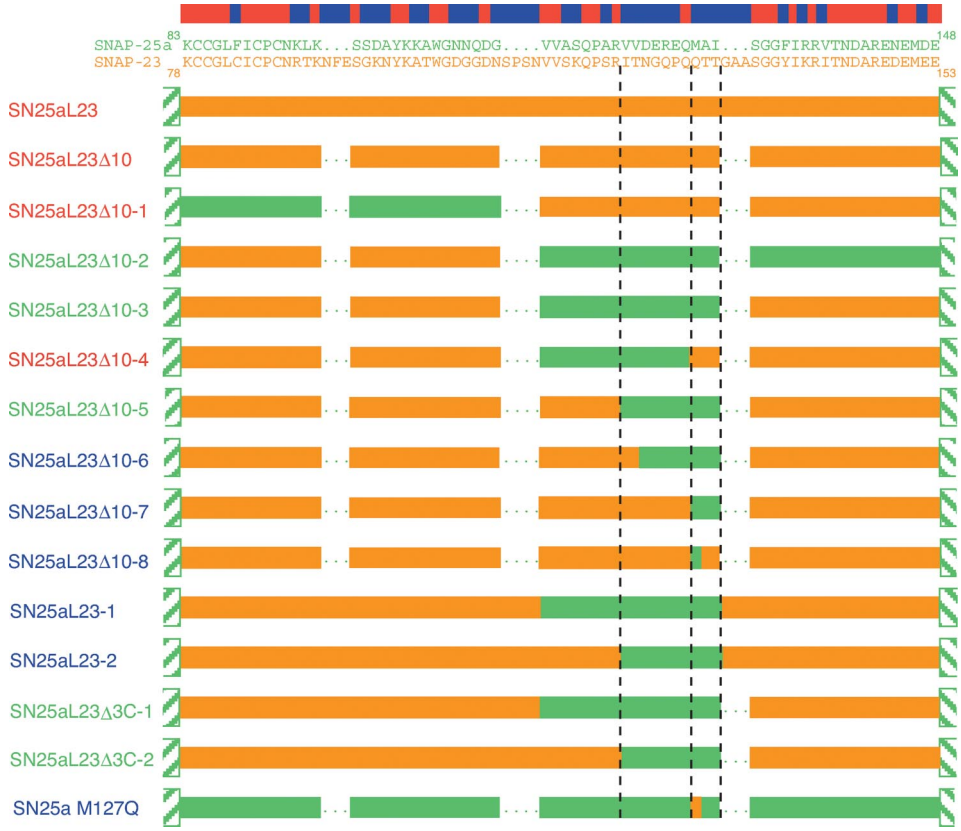

Figure 5. Overview of SNAP-25a/SNAP-23 chimeric constructs. SNAP-25 is depicted in green, SNAP-23 in orange. The sequences of the SNAP-25a and SNAP-23 linker domains are shown aligned, the color of the bar above indicates identical (red) and variant (blue) positions. The ends of the first and second SNARE domain are shown as hatched green boxes attaching to the linker domains. Gaps in the sequences are shown with dots. The names of the chimeras are shown to the left of the sequences, color-coded to show the secretory phenotype. Chimeras in green showed a secretory phenotype indistinguishable from SNAP-25a, red chimeras showed the linker phenotype, i.e., incomplete rescue and lower rate of exocytosis triggering at intermediate $[Ca^{2+}]_i$, which was partly overcome at higher concentrations, blue chimeras displayed an intermediate phenotype between the linker phenotype and SNAP-25a.

A chimeric protein where the two initial valines were substituted for the SNAP-23 residues isoleucine and threonine (SN25aL23Δ10-6) resulted in a construct with an intermediate phenotype between the linker phenotype and SNAP-25a (Figure 8A). With this construct, the normal amplitude of the exocytotic burst was recognizable, but the triggering rate was still somewhat decreased and also the sustained component of release was depressed. Therefore, the N-terminal hydrophobicity of the SNAP-25 domain is necessary for full rescue. Another chimera (SN25aL23Δ10-4) was created by substituting the last three amino acids of the stretch (MAI) with the uncharged SNAP-23 residues (QTT). This construct displayed the linker phenotype (Figure 8B); thus, the C-terminal part of the domain is absolutely necessary for fast exocytosis triggering.

Interestingly, a chimera where only the methionine-127 from SNAP-25 was substituted for the glutamine residue in the SNAP-23 linker (SN25aL23Δ10-8) sufficed to speed the secretion up compared with the linker phenotype, even though not quite as much as when all three C-terminal amino acids MAI were from SNAP-25 (SN25aL23Δ10-7, Figure 9, A and B). The latter construct restored the size of the

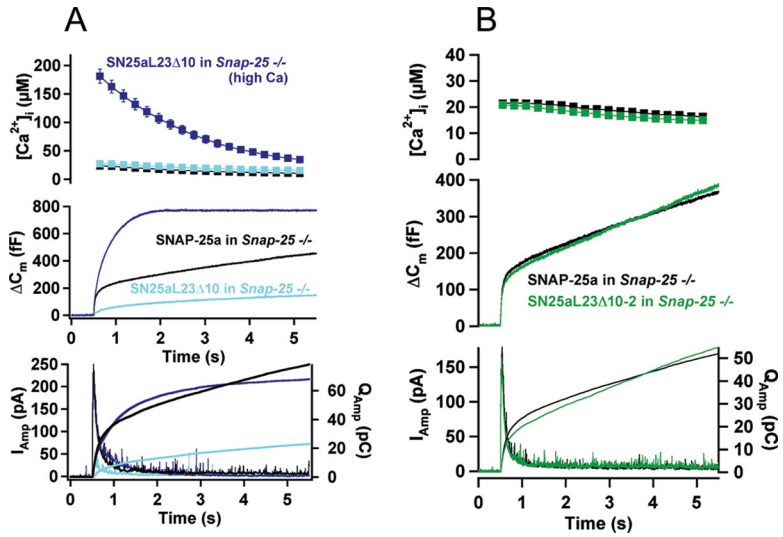

Figure 6. The second half of the SNAP-25 linker is necessary for fast exocytosis. (A) Secretion in the SN25aL23Δ10 chimera, in which the extra 10 amino acids in the SNAP-23 linker were deleted (see Figure 5). Exocytosis in the SN25aL23Δ10 chimera was depressed during stimulations to 20–30 μM $[Ca^{2+}]_i$ (light blue traces, n = 19 cells), but it is largely rescued as assayed by amperometry during flashes to higher $[Ca^{2+}]_i$ (blue traces, n = 20 cells). Note that the "overrescue" of the capacitance increase during stimulation to >100 μM is due to the fusion of vesicles that contain no catecholamines (see text for explanation). Therefore, only the amperometric trace contains information about the release of catecholamine-containing vesicles during high-$[Ca^{2+}]_i$ stimulation. For comparison is shown the rescue with WT SNAP-25a in *Snap25* −/− (black traces). (B) A chimera where the second half of the linker is from SNAP-25 (refer to Figure 5; SN25aL23Δ10-2) rescues secretion when expressed in *Snap-25* −/− (green traces, n = 22 cells) similar to WT SNAP-25a (black traces, n = 22 cells).

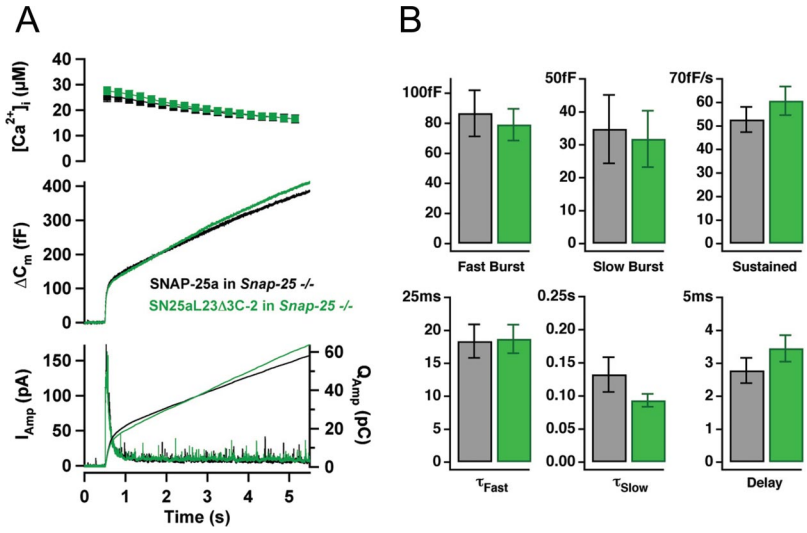

Figure 7. The minimum domain necessary for fast triggering encompasses amino acids 120–129 in SNAP-25. (A) A chimera where the amino acids 120–129 are from SNAP-25a (refer to Figure 5; SN25aL23Δ3C-2) rescues secretion to similar extent and kinetics as SNAP-25a (chimera: green traces, n = 22, SNAP-25a; black traces, n = 21). (B) Kinetic analysis of individual capacitance traces from measurements shown in A. The SN25aL23Δ3C-2 supported normal size of fast and slow burst, normal triggering rates and delays as well as a normal sustained rate of release.

burst, but still left time constants of triggering and the delay slowed down by a factor 2–4. Also the sustained component of release was depressed. This is interesting, because in this construct the proline-127 from SNAP-23 was present, and the central charges (DERE) in SNAP-25 were missing. Furthermore, the two chimeras where the last three amino acids (MAI) were from SNAP-25 (SN25aL23Δ10-6 and SN25aL23Δ10-7) displayed indistinguishable phenotypes (compare Figure 8A and Figure 9A), even though the former construct contained the middle charged stretch (DEREQ) from SNAP-25, whereas the latter had the SNAP-23 sequence (NGQPQ). Thus, both the C-terminal and N-terminal hydrophobicity of this stretch and especially methionine-127 is important for fast exocytosis triggering, whereas the middle stretch seems less important, because even a proline in this area does not impair secretion.

To investigate whether mutations in the domain from amino acid 120–129 changes exocytosis in the context of the full-length SNAP-25 protein, we generated the single point-mutation SNAP-25 M127Q (Figure 5). This single mutation sufficed to significantly increase the time constant of fast release and the secretory delay (Figure 9, C and D). In addition, the sustained component was reduced, even though this was not quite significant when testing with a Mann–Whitney test (Figure 9D). Thus, a mutation in the full-length SNAP-25a protein reproduces the main features of similar mutations in the context of the SNAP-23 linker.

Altogether, we conclude that the hydrophobicity of the N- and C-terminal ends of this linker domain is of critical importance for fast triggering, and the domain cannot be further subdivided without loosing functionality. Therefore, the 10 amino acids in the SNAP-25 linker from position 120–129 display the features of a single protein domain acting in fast exocytosis triggering.

DISCUSSION

A linker connecting the Qb and Qc SNARE domains is a unique feature of the exocytotic fusion pathway; however, no active role for the linker in exocytosis had been identified. Here, we show that the linker is intimately involved in fast Ca^{2+} triggering. Thus, this part of the SNARE complex warrants further attention.

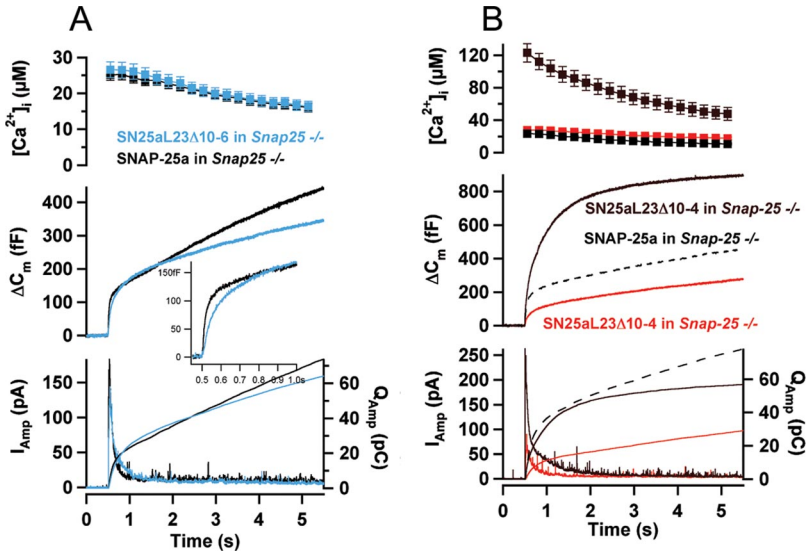

Figure 8. The hydrophobic part of the 10-amino acid stretch in SNAP-25 is critical for fast triggering. (A) A chimera (SN25aL23Δ10–6, blue traces, n = 25 cells) where the two initial valines of the critical stretch in SNAP-25 (VVDEREQMAI) were substituted for the SNAP-23 counterparts (IT) displays an intermediate phenotype characterized by slightly slower exocytosis triggering, and a reduced sustained component of release compared with SNAP-25a rescue (black trace, n = 26 cells). Inset, burst component (0.5–1 s) shown at higher resolution. (B) A chimera (SN25aL23Δ10-4, red and brown traces, n = 18 cells; compare with dotted black trace, SNAP-25a rescue) in which the three final amino acids of the critical stretch in SNAP-25 (MAI) were replaced by their SNAP-23 counterparts displayed the linker phenotype, i.e., impaired secretion at intermediate $[Ca^{2+}]_i$ (red traces), which was partially rescued at higher $[Ca^{2+}]_i$ (brown traces).

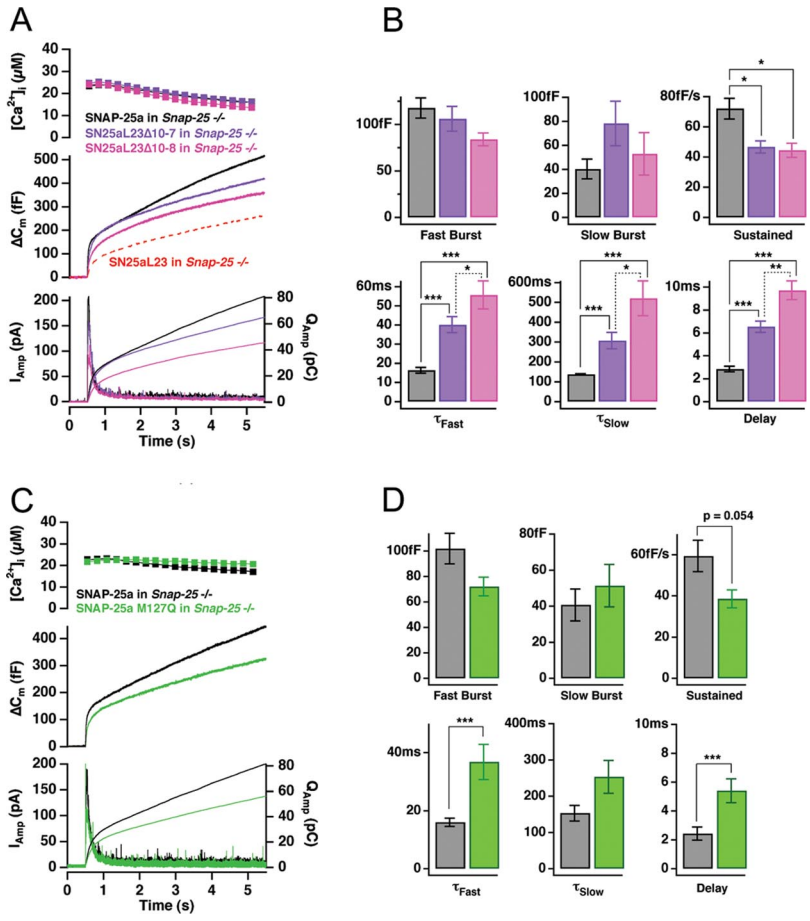

Figure 9. Subdividing the amino acid stretch 120–129 generates chimeras with intermediate phenotypes. (A) Overall secretion from a chimera where only the Methionine-127 was from SNAP-25 (SN25aL23Δ10–8, pink, n = 27) was increased compared with the SN25aL23 chimera (dotted red line shown only in the middle panel for comparison). A chimera where the amino acids 127–129 were from SNAP-25 (SN25aL23Δ10-7, mauve trace, n = 31) displayed even more secretion and an intact exocytotic burst (secretion until 0.5 s after the burst) even though the sustained phase of release was still slowed down compared with WT SNAP-25 (SNAP-25a, black, n = 40). (B) Kinetic analysis of secretion driven by WT SNAP-25a and the two chimera from A. The fast and slow burst sizes were not significantly changed in the chimeras, whereas the sustained component was significantly reduced. Furthermore, triggering rates and delays were gradually increased in the two chimeras, but still faster than in the linker chimera (SN25aL23, compare to Figure 3). (C) The single amino acid substitution M127Q in the SNAP-25a background (see Figure 5) suffices to slow down secretion (SNAP-25 M127Q, green, n = 26) compared with SNAP-25a rescue (SNAP-25a, black, n = 25). (D) Kinetic analysis of secretion driven by SNAP-25a M127Q (green) and WT SNAP-25a (black). Fusion of the fast burst was significantly slowed down, and the secretory delay prolonged in the mutant. The sustained phase of release showed a tendency toward a decreased rate (p = 0.054, Mann–Whitney test). Overall, kinetic changes were parallel to those seen in intermediate mutants made in the background of the SNAP-23 linker (compare with B). *p < 0.05, **p < 0.01, and ***p < 0.001 (Mann-Whitney test).

We analyzed the role of the palmitoylated cysteines in a null background, by expression in *Snap-25* knockout chromaffin cells. Our data confirm the function of the cysteines in targeting SNAP-25 to the plasma membrane (Hess *et al.*, 1992; Veit *et al.*, 1996; Lane and Liu, 1997; Gonzalo *et al.*, 1999; Vogel and Roche, 1999; Gonelle-Gispert *et al.*, 2000; Koticha *et al.*, 2002; Loranger and Linder, 2002; Kammer *et al.*, 2003), in which it acts in exocytosis by binding to the Q-SNARE partner syntaxin-1. Removing single cysteines reduced the amount of SNAP-25 on the plasma membrane to <50%, but it did not impair secretion, as previously shown in insulin-secreting cells (Gonelle-Gispert *et al.*, 2000). A SNAP-25 without cysteines was expressed at lower levels than WT protein, but still induced significant rescue. The resulting secretion was slowed down and the duration of the fusion pore increased. Thus, the cysteines are important for the speed of exocytosis. The observed rescue agree with the finding by several groups that nonpalmitoylated SNAP-25 can support membrane fusion in in vitro assays (Scales *et al.*, 2000b; Schuette *et al.*, 2004) or after infusion into BoNT/E-treated PC12 cells (Scales *et al.*, 2000b). The slow-down of secretion found here using high time-resolution methods would not have been noticeable in those intrinsically slow assays.

It has been suggested that SNAP-25 and SNAP-23 are differentially targeted to membrane rafts, due to the presence of an extra cysteine in SNAP-23 (Salaun *et al.*, 2005a,b). Others have failed to find SNAREs in lipid rafts (Lang *et al.*, 2001), but they identified cholesterol-dependent SNARE clusters in plasma membrane sheets. We showed that the secretory phenotype of a chimeric SNAP-25a construct where the N-terminal half of the linker—including all cysteines—was from SNAP-23 did not deviate from SNAP-25a in our assay. Thus the difference in secretory phenotype between SNAP-25 and SNAP-23, which was found after overexpression (Sorensen *et al.*, 2003b), cannot be due to a different arrangement of cysteines. Likewise, we found that the cysteine clusters of the two SNAP-25 splice variants are functionally equivalent (Nagy *et al.*, 2005). Nevertheless, it remains possible that at lower expression levels differential targeting of SNAP-25 and SNAP-23 could be functionally important.

Using chimeric proteins we identified a 10-amino acid stretch in the C-terminal half of the SNAP-25 linker, which is necessary for fast exocytosis triggering. This stretch begins immediately C-terminal of the minimal domain required for palmitoylation of SNAP-25 in vivo (Gonzalo *et al.*, 1999) and did not affect expression level or membrane targeting. It consists of hydrophobic and charged amino acids, whereas the stretch in SNAP-23 is hydrophilic, but uncharged. Testing of chimera underlined the importance of the hydrophobicity for functionality. This domain is conserved in SNAP-25 from zebrafish to human (Figure 10A), whereas in the fly and worm one or two of the initial hydrophobic amino acids are present together with the important methionine and one-three charges in the middle (Figure 10A). An interesting exception is formed by the sea urchin, where the critical methionine is replaced by a cysteine. Cysteines are quite hydrophobic, even when not palmitoylated. Limited structural studies performed using CD spectroscopy showed

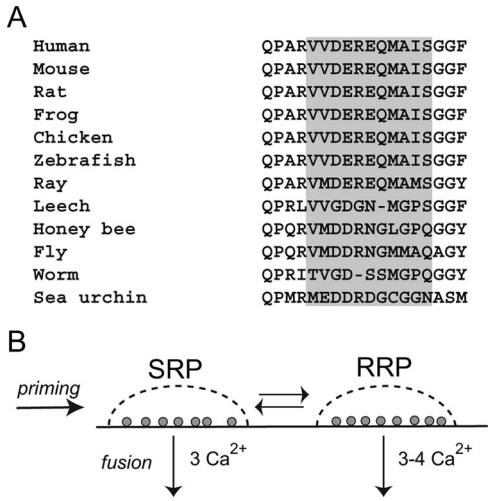

Figure 10. (A) Alignment of the critical linker domain in some SNAP-25 orthologues based on a recent classification (Kloepper *et al*., 2007). The 10 amino acids important for exocytosis triggering are marked by a shaded box. (B) Sequential model for exocytosis in the chromaffin cells. Vesicles become release-competent through the priming reaction (note that this reaction is assumed reversible, even though it for simplicity is shown with a single arrow). Primed vesicles can belong to the SRP, or the RRP. The RRP vesicles fuse ~10 times faster than SRP vesicles.

that both are unstructured in solution (Supplemental Figure 5), in agreement with previous data (Margittai *et al*., 2001). Also, our electrophysiological data indicate the lack of secondary structure, since replacing the middle part of the 10-amino acid stretch with residues from SNAP-23, which involved the insertion of a proline, did not further exacerbate the intermediate phenotype found upon replacement of the first two valines. Finally, the stretch is flanked to both sides by helix-breakers (prolines, glycines), making it unlikely that this domain would change the structure of the SNARE-domains through a *cis*-action.

The most remarkable effect of replacing the SNAP-25 linker with its SNAP-23 counterpart is a displacement of the calcium dependence of fast exocytosis triggering toward higher concentrations (Figure 3, G and H). This displacement also seems to affect vesicles fusing from the SRP (Figure 3, D and F). The ability of a SNAP-23 domain to displace the calcium-dependence toward higher values is surprising, because it was shown previously that SNAP-23 induce vesicle docking and fusion in N2A cells at low, resting, calcium levels (Chieregatti *et al*., 2004). However, Chieregatti *et al*. (2004) also showed that synaptotagmin-7 suppresses SNAP-23–induced basal release. Synaptotagmin-7 is expressed in and modulates secretion from chromaffin cells (Schonn *et al*., 2008). Thus, the ability of SNAP-23 to stimulate exocytosis under resting conditions depends on the expression of auxiliary proteins and/or the cell type.

In addition, we found that the rate of sustained release at high $[Ca^{2+}]_i$ was slowed down by the SNAP-23 linker (Figure 3, B and F). In a sequential model of exocytosis (Figure 10B), the priming rate can be measured from the sustained release component, but only if the fusion rate is kept much higher than the priming rate during the experiment. In the SN25L23 chimera, this assumption breaks down because of the dramatic slowdown of fusion triggering, which might have caused newly recruited vesicles to become "trapped" in the SRP. Simulations of the model in Figure 10B by using triggering rates estimated from Figure 3 showed that about half of the decrease in sustained component might be explained by the decrease in fusion triggering (data not shown), whereas the other half might represent a real depression of the vesicle priming reaction.

The displacement of the *intracellular* calcium dependence of exocytosis triggering is a very specific phenotype. Indeed, it is striking that the only molecular manipulations that are known—or are likely based on published literature—to change the intracellular calcium-dependence of exocytosis triggering are mutations in synaptotagmins and SNAP-25 (Sorensen *et al*., 2003a; Wang *et al*., 2003; Chieregatti *et al*., 2004; Rhee *et al*., 2005; Wang *et al*., 2005; Nagy *et al*., 2006; Pang *et al*., 2006; Sorensen *et al*., 2006). In contrast, manipulations of proteins involved in exocytosis more often lead to changes in pool sizes and/or recruitment in the absence of a change in triggering: examples include tomosyn (Yizhar *et al*., 2004), Munc13 (Ashery *et al*., 2000), Munc18 (Voets *et al*., 2001; Gulyas-Kovacs *et al*., 2007), CAPS1 (Speidel *et al*., 2005), SV2 (Xu and Bajjalieh, 2001), Snapin (Tian *et al*., 2005), synaptobrevin (Borisovska *et al*., 2005), and α-SNAP/NSF (Xu *et al*., 1999). Our present work extends the limited number of molecular manipulations that change the intracellular calcium dependence of exocytosis triggering to include the SNAP-25 linker.

There is ample evidence that synaptotagmin-1 binds to the SNARE complex or to individual SNAREs through interactions with one or both C2-domains (Bennett *et al*., 1992; Sollner *et al*., 1993; Chapman *et al*., 1995; Schiavo *et al*., 1997; Zhang *et al*., 2002; Rickman and Davletov, 2003; Shin *et al*., 2003; Bai *et al*., 2004; Bhalla *et al*., 2006; Pang *et al*., 2006; Lynch *et al*., 2007). It is possible that the SNAP-25 linker participates in synaptotagmin binding in situ. Another possibility, with would agree with the importance of the hydrophobic residues, is that the SNAP-25 linker affects interactions with the membrane that take place simultaneously with Ca^{2+} binding to synaptotagmin-1. Finally, the linker might affect stages of SNARE complex assembly, which could change both vesicle priming and fusion reactions (Sorensen *et al*., 2006), possibly by stabilizing an intermediate conformation of the SNARE complex (An and Almers, 2004). The picture emerging is that SNAREs, synaptotagmins, and lipids form an integrated fusion machine (Bhalla *et al*., 2006; Pang *et al*., 2006; Dai *et al*., 2007), whose calcium dependence is set by the properties of the entire assembly. The SNAP-25 linker must be seen as an integral part of this machine and it is tempting to speculate that the fusion of the Qb and Qc-SNARE motifs might have evolved as an adaptation toward calcium triggering of exocytosis.

ACKNOWLEDGMENTS

We thank Dirk Reuter and Ina Herfort for expert technical assistance, and Ralf B. Nehring for advice during the construction of the mutants. We are deeply indebted to Erwin Neher for ongoing discussions and support. We thank Dirk Fasshauer, Reinhard Jahn, and Josep Rizo for comments on an earlier version of the manuscript. This work was supported by Deutsche Forschungsgemeinschaft grant SFB523-B16 (to J.B.S.).

REFERENCES

An, S. J., and Almers, W. (2004). Tracking SNARE complex formation in live endocrine cells. Science *306*, 1042–1046.

Ashery, U., Betz, A., Xu, T., Brose, N., and Rettig, J. (1999). An efficient method for infection of adrenal chromaffin cells using the Semliki Forest virus gene expression system. Eur. J. Cell Biol. *78*, 525–532.

Ashery, U., Varoqueaux, F., Voets, T., Betz, A., Thakur, P., Koch, H., Neher, E., Brose, N., and Rettig, J. (2000). Munc13-1 acts as a priming factor for large dense-core vesicles in bovine chromaffin cells. EMBO J. *19*, 3586–3596.

Bai, J., Wang, C. T., Richards, D. A., Jackson, M. B., and Chapman, E. R. (2004). Fusion pore dynamics are regulated by synaptotagmin*t-SNARE interactions. Neuron *41*, 929–942.

Bennett, M. K., Calakos, N., and Scheller, R. H. (1992). Syntaxin: a synaptic protein implicated in docking of synaptic vesicles at presynaptic active zones. Science *257*, 255–259.

Bhalla, A., Chicka, M. C., Tucker, W. C., and Chapman, E. R. (2006). Ca(2+)-synaptotagmin directly regulates t-SNARE function during reconstituted membrane fusion. Nat. Struct. Mol. Biol. *13*, 323–330.

Borisovska, M., Zhao, Y., Tsytsyura, Y., Glyvuk, N., Takamori, S., Matti, U., Rettig, J., Sudhof, T., and Bruns, D. (2005). v-SNAREs control exocytosis of vesicles from priming to fusion. EMBO J *24*, 2114–2126.

Chapman, E. R., Hanson, P. I., An, S., and Jahn, R. (1995). Ca2+ regulates the interaction between synaptotagmin and syntaxin 1. J. Biol. Chem. *270*, 23667–23671.

Chieregatti, E., Chicka, M. C., Chapman, E. R., and Baldini, G. (2004). SNAP-23 functions in docking/fusion of granules at low Ca^{2+}. Mol. Biol. Cell *15*, 1918–1930.

Dai, H., Shen, N., Arac, D., and Rizo, J. (2007). A quaternary SNARE-synaptotagmin-Ca(2+)-phospholipid complex in neurotransmitter release. J. Mol. Biol. *367*, 848–863.

Fasshauer, D. (2003). Structural insights into the SNARE mechanism. Biochim. Biophys. Acta *1641*, 87–97.

Fasshauer, D., Eliason, W. K., Brunger, A. T., and Jahn, R. (1998a). Identification of a minimal core of the synaptic SNARE complex sufficient for reversible assembly and disassembly. Biochemistry *37*, 10354–10362.

Fasshauer, D., Sutton, R. B., Brunger, A. T., and Jahn, R. (1998b). Conserved structural features of the synaptic fusion complex: SNARE proteins reclassified as Q- and R-SNAREs. Proc. Natl. Acad. Sci. USA *95*, 15781–15786.

Fukuda, R., McNew, J. A., Weber, T., Parlati, F., Engel, T., Nickel, W., Rothman, J. E., and Sollner, T. H. (2000). Functional architecture of an intracellular membrane t-SNARE. Nature *407*, 198–202.

Gonelle-Gispert, C., Molinete, M., Halban, P. A., and Sadoul, K. (2000). Membrane localization and biological activity of SNAP-25 cysteine mutants in insulin-secreting cells. J. Cell Sci. *113*, 3197–3205.

Gonzalo, S., Greentree, W. K., and Linder, M. E. (1999). SNAP-25 is targeted to the plasma membrane through a novel membrane-binding domain. J. Biol. Chem. *274*, 21313–21318.

Gulyas-Kovacs, A., de Wit, H., Milosevic, I., Kochubey, O., Toonen, R., Klingauf, J., Verhage, M., and Sorensen, J. B. (2007). Munc18-1, sequential interactions with the fusion machinery stimulate vesicle docking and priming. J. Neurosci. *27*, 8676–8686.

Hess, D. T., Slater, T. M., Wilson, M. C., and Skene, J. H. (1992). The 25 kDa synaptosomal-associated protein SNAP-25 is the major methionine-rich polypeptide in rapid axonal transport and a major substrate for palmitoylation in adult CNS. J. Neurosci. *12*, 4634–4641.

Jackson, M. B., and Chapman, E. R. (2006). Fusion pores and fusion machines in Ca2+-triggered exocytosis. Annu. Rev. Biophys. Biomol. Struct. *35*, 135–160.

Jahn, R., and Scheller, R. H. (2006). SNAREs–engines for membrane fusion. Nat. Rev. Mol. Cell Biol. *7*, 631–643.

Kammer, B., Schmidt, M. F., and Veit, M. (2003). Functional characterization of palmitoylated and nonacylated SNAP-25 purified from insect cells infected with recombinant baculovirus. Mol. Cell Neurosci. *23*, 333–340.

Kloepper, T. H., Kienle, C. N., and Fasshauer, D. (2007). An elaborate classification of SNARE proteins sheds light on the conservation of the eukaryotic endomembrane system. Mol. Biol. Cell *18*, 3463–3471.

Koticha, D. K., McCarthy, E. E., and Baldini, G. (2002). Plasma membrane targeting of SNAP-25 increases its local concentration and is necessary for SNARE complex formation and regulated exocytosis. J. Cell Sci. *115*, 3341–3351.

Lane, S. R., and Liu, Y. (1997). Characterization of the palmitoylation domain of SNAP-25. J. Neurochem. *69*, 1864–1869.

Lang, T., Bruns, D., Wenzel, D., Riedel, D., Holroyd, P., Thiele, C., and Jahn, R. (2001). SNAREs are concentrated in cholesterol-dependent clusters that define docking and fusion sites for exocytosis. EMBO J. *20*, 2202–2213.

Loranger, S. S., and Linder, M. E. (2002). SNAP-25 traffics to the plasma membrane by a syntaxin-independent mechanism. J. Biol. Chem. *277*, 34303–34309.

Lynch, K. L., Gerona, R. R., Larsen, E. C., Marcia, R. F., Mitchell, J. C., and Martin, T. F. (2007). Synaptotagmin C2A Loop 2 Mediates Ca2+-dependent SNARE Interactions Essential for Ca2+-triggered Vesicle Exocytosis. Mol. Biol. Cell *18*, 4957–4968.

Margittai, M., Fasshauer, D., Pabst, S., Jahn, R., and Langen, R. (2001). Homo- and heterooligomeric SNARE complexes studied by site-directed spin labeling. J. Biol. Chem. *276*, 13169–13177.

McNew, J. A., Parlati, F., Fukuda, R., Johnston, R. J., Paz, K., Paumet, F., Sollner, T. H., and Rothman, J. E. (2000). Compartmental specificity of cellular membrane fusion encoded in SNARE proteins. Nature *407*, 153–159.

Nagy, G., Kim, J. H., Pang, Z. P., Matti, U., Rettig, J., Sudhof, T. C., and Sorensen, J. B. (2006). Different effects on fast exocytosis induced by synaptotagmin 1 and 2 isoforms and abundance but not by phosphorylation. J. Neurosci. *26*, 632–643.

Nagy, G., Matti, U., Nehring, R. B., Binz, T., Rettig, J., Neher, E., and Sorensen, J. B. (2002). Protein kinase C-dependent phosphorylation of synaptosome-associated protein of 25 kDa at Ser187 potentiates vesicle recruitment. J. Neurosci. *22*, 9278–9286.

Nagy, G., Milosevic, I., Fasshauer, D., Muller, E. M., de Groot, B. L., Lang, T., Wilson, M. C., and Sorensen, J. B. (2005). Alternative splicing of SNAP-25 regulates secretion through nonconservative substitutions in the SNARE domain. Mol. Biol. Cell *16*, 5675–5685.

Pang, Z. P., Shin, O. H., Meyer, A. C., Rosenmund, C., and Sudhof, T. C. (2006). A gain-of-function mutation in synaptotagmin-1 reveals a critical role of Ca2+-dependent soluble N-ethylmaleimide-sensitive factor attachment protein receptor complex binding in synaptic exocytosis. J. Neurosci. *26*, 12556–12565.

Rhee, J. S., Li, L. Y., Shin, O. H., Rah, J. C., Rizo, J., Sudhof, T. C., and Rosenmund, C. (2005). Augmenting neurotransmitter release by enhancing the apparent Ca2+ affinity of synaptotagmin 1. Proc. Natl. Acad. Sci. USA *102*, 18664–18669.

Rickman, C., and Davletov, B. (2003). Mechanism of calcium-independent synaptotagmin binding to target SNAREs. J. Biol. Chem. *278*, 5501–5504.

Rizo, J., Chen, X., and Arac, D. (2006). Unraveling the mechanisms of synaptotagmin and SNARE function in neurotransmitter release. Trends Cell Biol. *16*, 339–350.

Salaun, C., Gould, G. W., and Chamberlain, L. H. (2005a). Lipid raft association of SNARE proteins regulates exocytosis in PC12 cells. J. Biol. Chem. *280*, 19449–19453.

Salaun, C., Gould, G. W., and Chamberlain, L. H. (2005b). The SNARE proteins SNAP-25 and SNAP-23 display different affinities for lipid rafts in PC12 cells. Regulation by distinct cysteine-rich domains. J. Biol. Chem. *280*, 1236–1240.

Scales, S. J., Bock, J. B., and Scheller, R. H. (2000a). The specifics of membrane fusion. Nature *407*, 144–146.

Scales, S. J., Chen, Y. A., Yoo, B. Y., Patel, S. M., Doung, Y. C., and Scheller, R. H. (2000b). SNAREs contribute to the specificity of membrane fusion. Neuron *26*, 457–464.

Schagger, H., Aquila, H., and Von Jagow, G. (1988). Coomassie blue-sodium dodecyl sulfate-polyacrylamide gel electrophoresis for direct visualization of polypeptides during electrophoresis. Anal. Biochem. *173*, 201–205.

Schiavo, G., Stenbeck, G., Rothman, J. E., and Sollner, T. H. (1997). Binding of the synaptic vesicle v-SNARE, synaptotagmin, to the plasma membrane t-SNARE, SNAP-25, can explain docked vesicles at neurotoxin-treated synapses. Proc. Natl. Acad. Sci. USA *94*, 997–1001.

Schonn, J. S., Maximov, A., Lao, Y., Sudhof, T. C., and Sorensen, J. B. (2008). Synaptotagmin-1 and -7 are functionally overlapping Ca2+ sensors for exocytosis in adrenal chromaffin cells. Proc. Natl. Acad. Sci. USA *105*, 3998–4003.

Schuette, C. G., Hatsuzawa, K., Margittai, M., Stein, A., Riedel, D., Kuster, P., Konig, M., Seidel, C., and Jahn, R. (2004). Determinants of liposome fusion mediated by synaptic SNARE proteins. Proc. Natl. Acad. Sci. USA *101*, 2858–2863.

Shin, O. H., Rhee, J. S., Tang, J., Sugita, S., Rosenmund, C., and Sudhof, T. C. (2003). Sr2+ binding to the Ca2+ binding site of the synaptotagmin 1 C2B domain triggers fast exocytosis without stimulating SNARE interactions. Neuron *37*, 99–108.

Sollner, T., Bennett, M. K., Whiteheart, S. W., Scheller, R. H., and Rothman, J. E. (1993). A protein assembly-disassembly pathway in vitro that may correspond to sequential steps of synaptic vesicle docking, activation, and fusion. Cell *75*, 409–418.

Sorensen, J. B. (2004). Formation, stabilisation and fusion of the readily releasable pool of secretory vesicles. Pflugers Arch. *448*, 347–362.

Sorensen, J. B., Fernandez-Chacon, R., Sudhof, T. C., and Neher, E. (2003a). Examining synaptotagmin 1 function in dense core vesicle exocytosis under direct control of Ca2+. J. Gen. Physiol. *122*, 265–276.

Sorensen, J. B., Nagy, G., Varoqueaux, F., Nehring, R. B., Brose, N., Wilson, M. C., and Neher, E. (2003b). Differential control of the releasable vesicle pools by SNAP-25 splice variants and SNAP-23. Cell *114*, 75–86.

Sorensen, J. B., Wiederhold, K., Muller, E. M., Milosevic, I., Nagy, G., de Groot, B. L., Grubmuller, H., and Fasshauer, D. (2006). Sequential N- to C-terminal SNARE complex assembly drives priming and fusion of secretory vesicles. EMBO J. *25*, 955–966.

Speidel, D. *et al*. (2005). CAPS1 regulates catecholamine loading of large dense-core vesicles. Neuron *46*, 75–88.

Sutton, R. B., Fasshauer, D., Jahn, R., and Brunger, A. T. (1998). Crystal structure of a SNARE complex involved in synaptic exocytosis at 2.4 A resolution. Nature *395*, 347–353.

Terrian, D. M., and White, M. K. (1997). Phylogenetic analysis of membrane trafficking proteins: a family reunion and secondary structure predictions. Eur. J. Cell Biol. *73*, 198–204.

Tian, J. H. *et al*. (2005). The role of Snapin in neurosecretion: snapin knock-out mice exhibit impaired calcium-dependent exocytosis of large dense-core vesicles in chromaffin cells. J. Neurosci. *25*, 10546–10555.

Veit, M., Sollner, T. H., and Rothman, J. E. (1996). Multiple palmitoylation of synaptotagmin and the t-SNARE SNAP-25. FEBS Lett. *385*, 119–123.

Voets, T. (2000). Dissection of three Ca2+-dependent steps leading to secretion in chromaffin cells from mouse adrenal slices. Neuron *28*, 537–545.

Voets, T., Toonen, R. F., Brian, E. C., de Wit, H., Moser, T., Rettig, J., Sudhof, T. C., Neher, E., and Verhage, M. (2001). Munc18-1 promotes large dense-core vesicle docking. Neuron *31*, 581–591.

Vogel, K., and Roche, P. A. (1999). SNAP-23 and SNAP-25 are palmitoylated in vivo. Biochem. Biophys. Res. Commun. *258*, 407–410.

Wang, C. T., Lu, J. C., Bai, J., Chang, P. Y., Martin, T. F., Chapman, E. R., and Jackson, M. B. (2003). Different domains of synaptotagmin control the choice between kiss-and-run and full fusion. Nature *424*, 943–947.

Wang, P., Chicka, M. C., Bhalla, A., Richards, D. A., and Chapman, E. R. (2005). Synaptotagmin VII is targeted to secretory organelles in PC12 cells, where it functions as a high-affinity calcium sensor. Mol. Cell. Biol. *25*, 8693–8702.

Washbourne, P., Cansino, V., Mathews, J. R., Graham, M., Burgoyne, R. D., and Wilson, M. C. (2001). Cysteine residues of SNAP-25 are required for SNARE disassembly and exocytosis, but not for membrane targeting. Biochem. J. *357*, 625–634.

Weimbs, T., Low, S. H., Chapin, S. J., Mostov, K. E., Bucher, P., and Hofmann, K. (1997). A conserved domain is present in different families of vesicular fusion proteins: a new superfamily. Proc. Natl. Acad. Sci. USA *94*, 3046–3051.

Weimbs, T., Mostov, K., Low, S. H., and Hofmann, K. (1998). A model for structural similarity between different SNARE complexes based on sequence relationships. Trends Cell Biol. *8*, 260–262.

Xu, T., Ashery, U., Burgoyne, R. D., and Neher, E. (1999). Early requirement for alpha-SNAP and NSF in the secretory cascade in chromaffin cells. EMBO J. *18*, 3293–3304.

Xu, T., and Bajjalieh, S. M. (2001). SV2 modulates the size of the readily releasable pool of secretory vesicles. Nat. Cell Biol. *3*, 691–698.

Xu, T., Binz, T., Niemann, H., and Neher, E. (1998). Multiple kinetic components of exocytosis distinguished by neurotoxin sensitivity. Nat. Neurosci. *1*, 192–200.

Yizhar, O., Matti, U., Melamed, R., Hagalili, Y., Bruns, D., Rettig, J., and Ashery, U. (2004). Tomosyn inhibits priming of large dense-core vesicles in a calcium-dependent manner. Proc. Natl. Acad. Sci. USA *101*, 2578–2583.

Zhang, X., Kim-Miller, M. J., Fukuda, M., Kowalchyk, J. A., and Martin, T. F. (2002). Ca2+-dependent synaptotagmin binding to SNAP-25 is essential for Ca2+-triggered exocytosis. Neuron *34*, 599–611.